Short Papers

The Vector-Gradient Hough Transform

Rita Cucchiara and Fabio Filicori

Abstract—The paper presents a new transform, called *Vector–Gradient Hough Transform*, for identifying elongated shapes in gray-scale images. This goal is achieved not only by collecting information on the edges of the objects, but also by reconstructing their transversal profile of luminosity. The main features of the new approach are related to its vector space formulation and the associated capability of exploiting all the vector information of the luminosity gradient.

Index Terms—Hough transform, shape detection, visual inspection, feature extraction, image analysis, object recognition.

1 Introduction

A great deal of scientific interest has been focused on the *Hough transform* (HT) and its derived formulations, for detecting and identifying parametric curves in images [5], [7]. Mainly, the HT is used as an extractor of low-level primitives (like, for instance, straight edges) for shape analysis purposes. In addition to the HT for straight lines [5] and for basic parametric curves, many other specific shape models and corresponding HT-based approaches have been proposed. Examples are the *ISLS* (Ideal Straight Line Segment) for recognizing bar segments [1], the *PWCS* used with the Distributed HT for circular patterns [8] and the *STIRS* signature for a generic curve adopted with the Straight Line HT [10]. In general, these models characterize some geometrical aspects of objects in terms of 1D curves, by assuming that 2D shapes may by identified by their 1D (often binarized) edges.

When a more detailed shape model has to be adopted in order to consider the image points in their gray-level scale, HT-based approaches normally exploit the gradient of the luminosity function, according to the widely used Gradient Weighted Hough Transform (GWHT) [6], [12].

In such a context, we propose a new HT-based technique for shape detection in gray level images. The method is oriented to a class of elongated and almost rectilinear objects, whose nonnegligible luminosity variations also in the shorter dimension are shape-characterizing and thus must be identified and possibly reconstructed. We call this class of shapes *Straight-Translation-Generated Shape* (STGS) since the target objects may be thought to be generated by a straight translation in the 2D space of a 1D luminosity profile. In order to formally define the STGS model, we consider a 1D luminosity function, that is a generator profile of luminosity $\varphi(\xi)$ given in a 1D positive axis x' with $\xi > 0$. If the x' axis is rotated at an angle β with respect to the axis x of a 2D Cartesian space (x, y), the model of the STGS is defined by a function $f(x, y)$ generated by the straight translation of $\varphi(\xi)$ along a direction y' normal to x'. Thus the STGS is defined by

$$f(x, y) = \varphi(\xi)$$

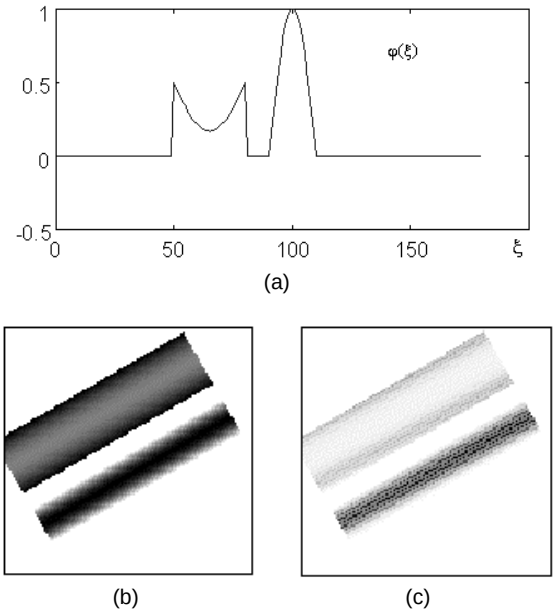

Fig. 1. An example of STGS shape. (a) The generator profile $\phi(\xi)$. (b) The generated image $f(x, y)$. (c) The reconstructed image after the identification process.

where

$$\xi = x\cos(\beta) + y\sin(\beta) \quad (1)$$

If the 2D Cartesian space is the image space, $f(x, y)$ represents the luminance function associated to the target STGS object. Fig. 1 gives a graphic example, showing a 1D generator profile (Fig. 1a) and the corresponding image $f(x, y)$ generated after a rotation of an angle $\beta = 30^\circ$ (Fig. 1b).

The 2D image space can also be viewed as a *vector space*, after introducing two unit vectors $\hat{i}$ and $\hat{j}$ along the axes, where a point (x, y) is identified by the corresponding vector $\mathbf{s}(x, y) = x\hat{i} + y\hat{j}$. In the same way, the luminosity gradient can be described in its vector form as

$$\mathbf{g}(\mathbf{s}) = \left(\partial f/\partial y\right)\hat{i} + \left(\partial f/\partial y\right)\hat{j}.$$

The $\mathbf{g}(\mathbf{s})$ vector can also be identified by its magnitude $G(\mathbf{s})$ and the associated angle $\gamma(\mathbf{s})$ with $\gamma \in [0, 2\pi[$. According to the STGS model in (1), all points of the object belonging to the same translation line should have the same luminosity value and the same gradient vector (i.e., with equal magnitude and direction). Many 2D shapes can be described by this model, either as templates of real objects or elongated light spots, patterns, or extended textures. Typical objects matching the STGS model are bar shapes, that can be thought of as generated by a finite translation of a rectangular 1D profile. Moreover, also less regular real-world shapes may be approximated by the STGS, such as those in Fig. 2, showing cracks and scratches on metallic surfaces.

The aim of the paper is to propose a new formulation of the Hough transform, called *Vector-Gradient Hough Transform* (VGHT) which, in addition to providing line location and orientation as the standard HT, enables the identification of STGS by detecting and reconstructing the transversal generator profile too.

2 The Vector-Gradient Hough Transform

The VGHT is a transformation from the image vector space, where $\mathbf{s}$ and $\mathbf{g}(\mathbf{s})$ are defined, into a vector parametric space. Each point of

- *R. Cucchiara is with Dipartimento di Ingegneria, Università di Ferrara, via Sargat 1, 44100 Ferrara, Italy. E-mail: rcucchiara@ing.unife.it.*
- *F. Filicori is with D.E.I.S., Università di Bologna, via Risorgimento 1, 410136 Bologna, Italy. E-mail: ffilicori@deis.unibo.it.*

Manuscript received 17 July 1996; revised 13 May 1998. Recommended for acceptance by R. Chin.
For information on obtaining reprints of this article, please send e-mail to: tpami@computer.org, and reference IEEECS Log Number 106859.

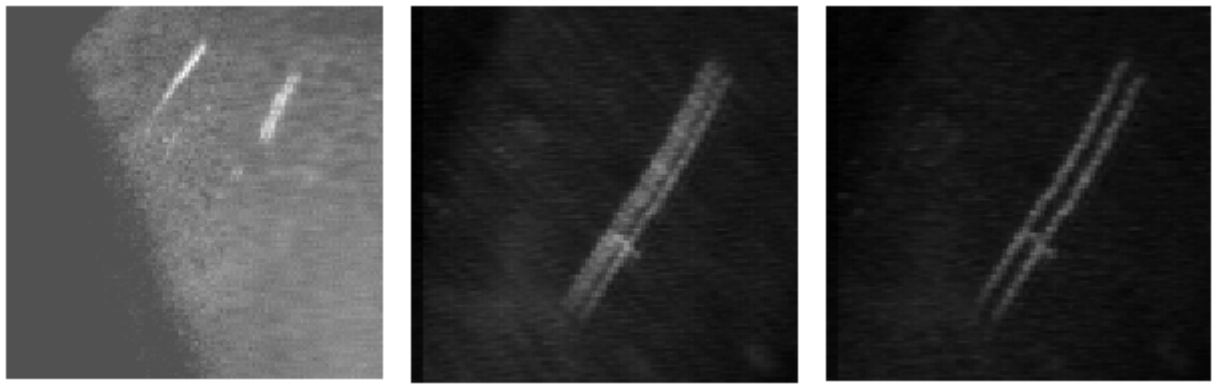

(a) (b) (c)

Fig. 2. Example of images: (a) IM0, (b) IM1, (c) IM2.

the transformed space is a vector **u**, represented by its polar coordinates (r, ϑ). We define the associated transform value, $\Gamma(\mathbf{u})$, as

$$\Gamma(\mathbf{u}) = VGHT(\rho, \vartheta) =$$

$$\int \left(\mathbf{g}(\mathbf{s}) \bullet \frac{\mathbf{u}}{|\mathbf{u}|} \right) \delta\left(|\mathbf{u}| - \mathbf{s} \bullet \frac{\mathbf{u}}{|\mathbf{u}|} \right) D\left(1 - \left| \frac{\mathbf{u} \bullet \mathbf{g}(\mathbf{s})}{|\mathbf{u}| \cdot |\mathbf{g}(\mathbf{s})|} \right| \right) ds \qquad (2)$$

where • represents the scalar product operator; $\delta(\cdot)$ is the Dirac impulse function, while $D(\alpha)$ is a finite version of it, i.e., a finite window function equal to $1/\Delta\epsilon$ if $\alpha \in [-\Delta\epsilon/2, \Delta\epsilon/2]$ and 0 otherwise.

In practice, the two Dirac operators select those points of the image space giving a nonzero contribution to the integral: since **u** can be written as $\mathbf{u} = r\left(\cos(\vartheta)\hat{i} + \sin(\vartheta)\hat{j}\right)$, the first Dirac term is not zero if its argument is null, i.e., if $r - r(\cos(\vartheta) + \sin(\vartheta))/r = 0$. Therefore, the first condition for a point $\mathbf{s}(x, y) = x\hat{i} + y\hat{j}$ to be taken into account in the integral is that

$$r = (x\cos(\vartheta) + y\sin(\vartheta)) \qquad (3)$$

If we consider the limit case of $lim\Delta\epsilon \to 0$, i.e., $D(\cdot) = \delta(\cdot)$, the second Dirac term is not null if and only if $\frac{rG\cos(\vartheta - \gamma)}{rG} = \pm 1$. This condition is satisfied when

$$\gamma = \vartheta + k\pi \qquad k = 0, \pm 1, \pm 2\ldots \qquad (4)$$

The former condition states that for a given **u**, the VHGT transform integrates gradient weighted values only from *collinear* image points, that is those satisfying (3). For the latter condition, only points with a vector gradient of the same direction as **u** (apart from the $k\pi$ term in (4)) contribute to the integral.

We call the transform *Vector-Gradient Hough Transform* (VGHT) since it exhibits many similarities with the gradient-weighted HT, while keeping all the vector proprieties of the gradient of the luminosity function. The VGHT can be used, like the other HT-based operators, for accumulating weighted "votes" in the transformed space, where peak detection identifies the parametric curve. However, in addition to detecting lines corresponding to straight edges in gray-levels images, VGHT also enables the 1D transversal profile of luminosity to be reconstructed and thus allows for a complete STGS identification.

3 Comparing VGHT and GWHT

In this section, we outline several features of VGHT by a comparison with the well-known GWHT [6]. The GWHT integrates *votes* of image points: unlike the basic HT, each image point (x, y) "votes" proportionally to its gradient magnitude and only for the angle of the gradient direction $\gamma(x, y)$.

For easier comparison, it should be noted that the standard HT for lines has been shown to be a particular case of the Radon transform [4] and defined in its integral form; also the GWHT can be expressed as

$$GWHT(x, y) =$$

$$\iint G(x, y)\delta(\rho - x\cos(\vartheta) - y\sin(\vartheta))\delta(\vartheta - \gamma(x, y))dxdy \qquad (5)$$

Beyond the formal differences due to the adoption of a vector representation in (2), the VGHT and the GWHT have some points in common: In both transforms, the integral weight is a function of the gradient and the point selection is based on the collinearity constraint defined by (3). Nevertheless, many substantial differences can be pointed out:

1) *Different transformed space:* The VGHT is defined over a vector space described by the polar coordinates $\vartheta \in [0, 2\pi[$ and r which is intrinsically nonnegative since represents the *Euclidean* distance computed by (3). Thus, the r coordinate ranges the interval $[0, R]$, with $R = \sqrt{(2)}I$ (for an image of I^2 pixels). Instead, the GWHT space is described by the same angular coordinate $\vartheta \in [0, 2\pi[$, but by the *algebraic* coordinate $\rho \in [-R, R]$ (i.e., with both positive and negative values) derived from the parametric straight line equation [6]. As an example, the VGHT and GWHT spaces related to the image IM1 are shown in Fig. 3 and Fig. 4, respectively. In both spaces, the two highest local extrema identify the two main straight edges of the crack; both peaks have a positive r coordinate in the VGHT space while have an opposite ρ sign in the GWHT space. By using the same discretizing grid (dr, da), the implementation of VGHT needs half the memory space with respect to that required by the conventional approach.
2) *Different angle selective operator:* In GWHT an image point (x, y) votes only for the angle $\vartheta = \gamma(x, y)$. Instead, VGHT selects two possible angles $\vartheta' = \gamma(x, y)$ and $\vartheta'' = (\gamma(x, y) + \pi)$ $mod(2\pi)$; however, the point votes for only one between ϑ' and ϑ'' owing to the constraint of $r \geq 0$. This original feature enhances the correlation between parallel "wavefronts" of luminosity variations, like the main parallel edges of objects modeled as STGS: In fact, two sets of collinear points with the same direction of the gradient but with the opposite sign (as the main edges of the cracks in Fig. 2) generate in the VGHT space local extrema at the same angle (see Fig. 3). Instead, in GWHT they produce two local peaks having the ρ coordinates with opposite sign and the angular coordinates with a π displacement (see Fig. 4).

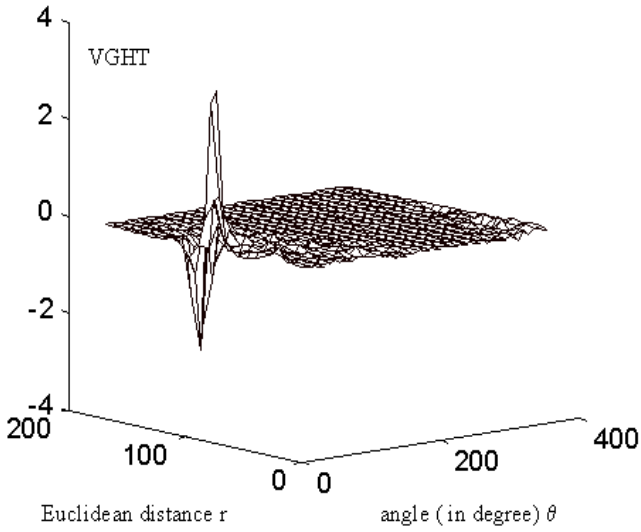

Fig. 3. VGHT for image IM1.

3) *Different integral weight:* The most important difference is the presence in VGHT of the scalar product $\mathbf{g}(\mathbf{s}) \bullet \frac{\mathbf{u}}{|\mathbf{u}|}$, implying that the weight of any voting point is given by $G(x, y)\cos(\gamma - \vartheta)$ instead of simply $G(x, y)$ as in GWHT. This involves the presence of a *signed* weight in VGHT: its positive or negative sign corresponds to the concordance or not of the gradient angle γ and the angle ϑ, i.e., the angle of the **u** vector considered, which identifies the possible direction where a set of "collinear" points could be detected. Therefore the VGHT points out, directly through its sign, the relationship between rising and falling variations of luminance in the same direction, while the same information is lost in GWHT, or can be partially retrieved through a post-processing phase only [12].

In conclusion, VGHT operates a sort of "double-mirroring" of GWHT (with symmetry axes $\rho = 0$ and $\vartheta = \pi$) balanced by a sign change: In particular, the same peaks associated to a decreasing (with respect to the axis origin) luminance function, which arise in the range $[\pi, 3/2\pi[$ of ϑ when using GWHT, are located in the range $[0, \pi[$, when using VGHT.

However, peak detection in VGHT space exhibits an enhanced discriminating capability with respect to that in GWHT space, since by using VGHT shape edges corresponding to increasing or falling luminance variations can easily be distinguished. In fact, if two peaks $\mathbf{u_1}$ and $\mathbf{u_2}$ are detected in VGHT at the polar coordinates (r_1, ϑ_1) and (r_2, ϑ_2), with the same angle, $\vartheta_1 = \vartheta_2$ and ordered with r ($r_1 < r_2$), the presence of a possible straight-edged object is detected by the condition $\Gamma(\mathbf{u_1}) \cdot \Gamma(\mathbf{u_2}) < 0$.

This feature enables a "real" object to be distinguished from other shapes with two edges with the same sign of the luminosity variation (e.g., the spot between an object's edge and the edge of its shadow where $\Gamma(\mathbf{u_1}) \cdot \Gamma(\mathbf{u_2}) > 0$). Moreover, dark shapes on a bright background or bright shapes on a dark background can be distinguished by verifying if a peak has either $\Gamma(\mathbf{u_1}) > 0$ or $\Gamma(\mathbf{u_1}) < 0$, respectively. Actually, the VGHT sign may cause a loss of information in some special cases, due to the integral nature of the HT, whenever two edges with equal length, equal gradient magnitude but opposite direction are exactly collinear. Conversely, the sign is essential for univocally identifying STGS objects, as will be pointed out in the next section.

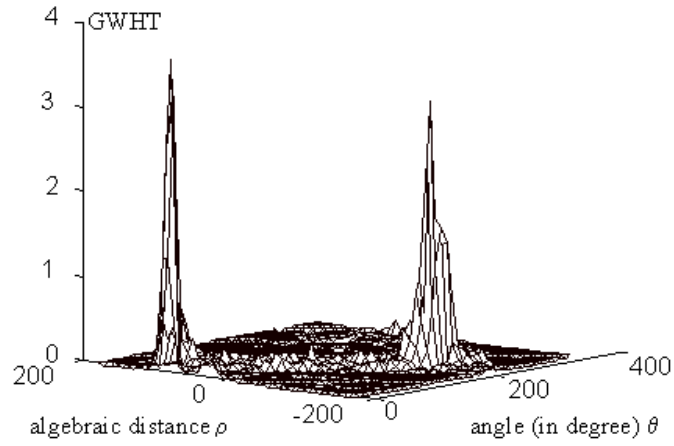

Fig. 4. GWHT for image IM1.

Up to now, an ideal Dirac operator $\delta(\cdot)$, instead of its practical finite version $D(\cdot)$, has been considered for a primarily VGHT evaluation. Instead, by exploiting the finite $D(\cdot)$ operator, the VGHT provides a more effective matching also with nonideal shapes. This operator accepts an angular displacement $\Delta\alpha$ between the local gradient and the **u** directions. In particular, the argument of the VGHT integral at a point $\mathbf{u}(r, \vartheta)$ becomes $G(x, y)\cos(\gamma(x, y) - \vartheta)$ if $r = x\cos\vartheta + y\sin\vartheta$ and $\vartheta = \gamma(x, y) + k\pi \pm \Delta\alpha$ (with k as defined in (4)) or 0 otherwise. The $D(\cdot)$ operator acts as a filtering on the angles in order to smooth the effects of small variations of the gradient direction between "collinear" points of the image. This operation is similar to many other smoothing operations, as for instance the one proposed in [11]. In our case, the adoption of the cosine-weighted operator, instead of a simple averaging as in [11], may make the transform slightly more angle-selective. However, this marginal benefit is not the reason for introducing the more computationally expensive cosine operator, which has been adopted with the main aim of exploiting also the sign information in the transform.

4 Identifying STGS With VGHT

The VGHT features outlined allow for a more efficient correlation of selected points in the transformed space and a more immediate detection of peaks, corresponding to straight edges in the image space. However, the peculiar aspect of VGHT is its capability of characterizing more complex shapes, as those modeled by STGS. In fact, it can be shown that if an image matches the STGS model, i.e., its luminance function $f(x, y)$ satisfies (1) for a given profile $\varphi(\xi)$ and an angle β, the VGHT transformed value at the point $\mathbf{u}(r, \beta)$ is proportional to the first-order directional derivative of the luminosity function along the β direction of the generator profile. That is,

$$\Gamma(\mathbf{u}\beta) = VGHT(r, \beta) = c(\partial\varphi(\xi)/\partial\xi)|_r$$

where the multiplying factor c is proportional to the translation length [3].

This propriety suggests the idea of associating with the VGHT, which has a differential meaning since it has the dimensions of gradients, another transform operator which has the dimensions of a luminosity function and is obtained by direct integration, without any previous peak detection, in the VGHT space. This leads to IVGHT (*Integrated VGHT*) defined as

$$\Gamma_I(\mathbf{u}(r, \vartheta)) = \int_0^r \Gamma(\mathbf{u}(a, \vartheta))da \qquad (6)$$

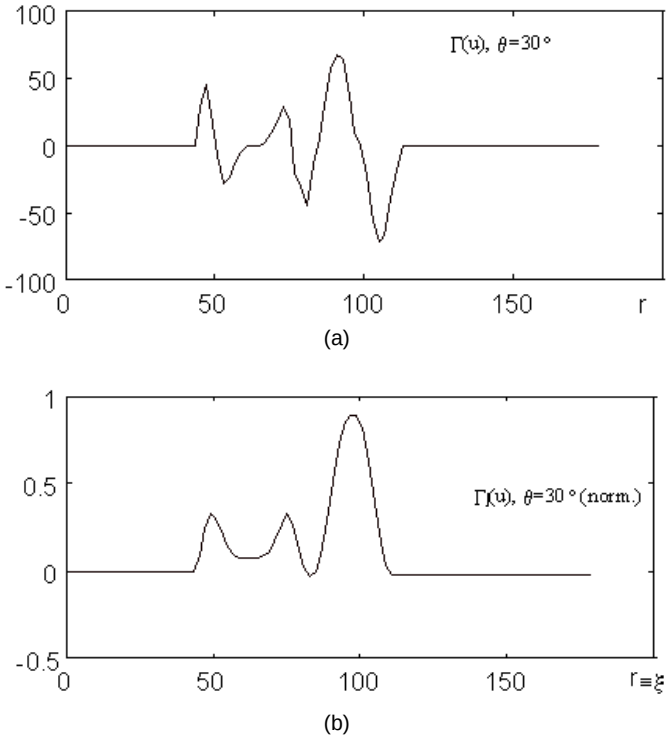

Fig. 5. (a) VGHT and (b) IVGHT for Fig. 1b ($0 < r < R$ and $\vartheta = 30^{\circ}$).

The $\Gamma_J(\mathbf{u}(r,\vartheta))$ value is, in practice, the sum of the luminance values of all the image points which ideally lie on a straight line whose foot[1] is identified by $\mathbf{u}$ and whose gradient direction coincides with that defined by ϑ. The IVGHT feature is outlined by the example in Fig. 5, showing the VGHT and IVGHT sections of the synthetic image in Fig. 1b, with a given angle $\vartheta = 30^{\circ}$ (equal to the β rotation of the profile of Fig. 1a). Thus, apart from truncation errors due to the discretization, the IVGHT is the reconstruction of the generator profile of the STGS model; on such a basis, an adequate back-projection enables the source image to be reconstructed. Fig. 1c is the back-projection of the extracted profile in Fig. 5b.

Therefore, by adopting the VGHT and IVGHT, not only can the edge points be detected by the corresponding peaks, but also all the bright points of an STGS-like object between the rising and falling luminance variations are identified. Fig. 6 shows the IVGHT space for IM1 of Fig. 2b. Both the amplitude and the shape of peaks in the IVGHT space are meaningful: In fact, while its spread along the angular direction shows the angular deviation of the translation direction from an ideal straight line, its spread along the r coordinate is a measure of the width of the luminosity generator profile and thus of the object thickness.

As an example of application, we present the use of the (I)VGHT for a highly selective quality inspection task, namely the detection and identification of cracks or scratches on metallic surfaces.

These defects are bright, elongated visual objects with steep contour edges, mainly straight (or with a very low curvature) and very close to each other due to the object thinness. These shapes appear to have been generated by translation of a 1D impulse of brightness in its normal direction, according the STGS model. Different transversal profiles produce different shapes: In Fig. 2, IM0 shows two "large and short" cracks, produced by translation of two separate profiles. Instead, IM1 and IM2 show a single and a

1. The *foot* of a line is intended as the intersection point between the line and its normal from the axes origin.

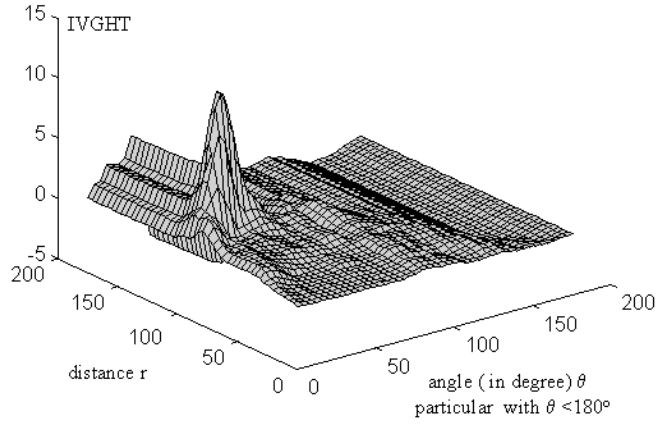

Fig. 6. IVGHT for image IM1 (particular with $0 < \vartheta < 180^{\circ}$).

double surface scratch, respectively: they can be modeled as STGSs characterized by different shaped generator profiles: the former by a single larger profile, while the latter by a sequence of two shorter pulses.

Accurate crack detection and identification criteria should be capable of distinguishing between these shapes, by also reconstructing the generator profile. This task can be carried out by VGHT followed by a local maxima detection, in order to find at least one of the peaks, possibly corresponding to an edge of a defect. Then, the defect detection is validated by the presence of another peak on the same angular coordinate but with the opposite sign (corresponding to the parallel complementary edge). Finally, the classification is carried out by the analysis of the IVGHT space in the neighborhood of the points where peaks have been detected, as the shape of the $\Gamma_J(\mathbf{u})$ reveals the generator profile.

The same kind of classification is not always possible with GWHT: In some cases, the presence of the pair of peaks may be deduced only after a specific post-processing aimed at verifying a correlation between peaks, which could be located at a displacement of π. However, since peak detection is normally carried out by peak ordering followed by appropriate peak selection, or by a thresholding operation on the peak amplitude [7], local peaks with a relatively low amplitude are not selected; therefore, some target objects, such as for instance the double scratch of IM2, whose inner pair of edges generate a couple of low amplitude peaks in the Hough space, are not detected by GWHT. Thus GWHT is not capable of discriminating between a large scratch and a double scratch, while this goal can be achieved by IVGHT. Fig. 7 shows the values of VGHT and IVGHT sections along the r direction for the angle where the highest peak has been found in VGHT. Fig. 7a and 7b refer to the single scratch of IM1 while Fig. 7c and 7d to the double scratch of IM2. The shape of the IVGHT profiles can be easily classified according to the specific requirements. This IVGHT approach is currently applied in an on-line fully automated industrial prototype for detecting and identifying cracks and scratches in the produced metallic objects.

5 Conclusion

The Vector-Gradient Hough transform has been proposed for identifying elongated and almost rectilinear shapes. The new approach exploits all the information associated to the vector formulation of the luminosity gradient, by introducing in the Hough transform a new angle selective operator and a signed weight function of the gradient magnitude. This intrinsic feature enhances the selectivity of peak detection for identifying collinear edge points in gray level images. However, the most peculiar feature of VGHT is the possibility, after an adequate integration of

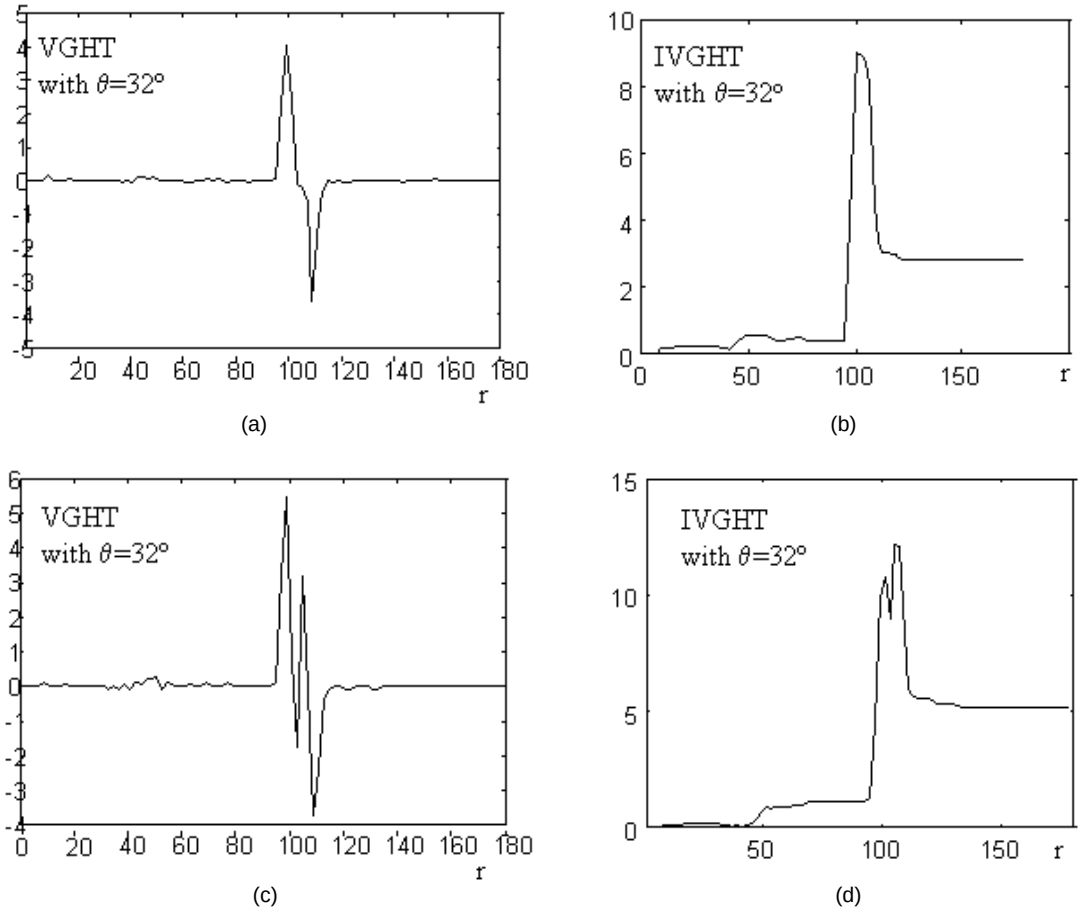

Fig. 7. Profiles reconstructed of IM1 and IM2. (a) and (c) VGHT sections for IM1 and IM2 at the angle of the highest peak. (b) and (d) IVGHT sections for IM1 and IM2 at the same angle.

the transformed space, of fully characterizing detected target shapes by also extracting their transversal luminosity profiles. This is made possible by the capability of the VGHT space to keep in each single angular coordinate all the information associated with the luminosity variation in the image space along that direction.

From the computational point of view, VGHT and GWHT have the same computational complexity $O(N)$, as $N = I^2$ is the image space cardinality. In practice, the algorithm for computing VGHT recalls the GWHT one and adds only a conditional branch which selects the angle, either $\gamma(x, y)$ or $(\gamma(x, y) + \pi)$ $mod(2\pi)$ as in (4), so as to have a positive r in (3). Therefore, due to the practical computational equivalence between the two approaches, all the considerations on discretization effects and the alternative algorithms for HT accumulation proposed for GWHT [7], [12], can be easily extended also to VGHT.

ACKNOWLEDGMENT

The research is found by an Italian Government Project MURST 40 percent and by a research contract with industry: "Integrity Defects Identification in Hot-Pressed Material"(Prot. n. 18998).

REFERENCES

[1] L. da Fontoura Costa, M.B. Sandler, "Effective Detection of Digital Bar Segments with Hough Transform," *CVGIP Computer Vision, Graphics, and Image Processing*, vol. 55, no. 3, pp. 180-191, 1993.

[2] R. Cucchiara and F. Filicori, "A Highly Selective HT based Algorithm for Detecting Extended, Almost Rectilinear Shapes," *Computer Analysis of Images and Patterns: LNC*, no. 970, pp. 692-698. Springer Verlag, 1995.

[3] R.Cucchiara and F.Filicori, "The Vector Gradient Hough Transform for Detecting Straight Translated Shapes," Tech Rep., no. 33 Dipartimento di Ingegneria, Univ. of Ferrara, Italy, June 1996.

[4] S.R. Deans, "Hough Transform From the Radon Transform," *IEEE Trans. Pattern Analysis and Machine Intelligence*, vol. 3, no. 2, Mar. 1981.

[5] R.O. Duda and P.E. Hart, "Use of the Hough Transform to Detect Lines and Curves in Pictures," *Comm. ACM*, vol. 15, pp. 11-15, 1972.

[6] F. O'Gorman and M.B. Clowes, "Finding Picture Edges Through Collinearity of Feature Points," *IEEE Trans. Computers*, vol. 25, no. 4, pp. 449-456, 1976.

[7] J. Illingworth and J. Kittler, "A Survey of the Hough Transform," *CVGIP Computer Vision, Graphics, and Image Processing*, vol. 43, pp. 221-238, 1988.

[8] J.N. Huddleston and J. Ben Arie, "Grouping Edgels Into Structural Entities Using Circular Symmetry: The Distributed Hough Transform and Probabilistic Non Accidentalness," *CVGIP Computer Vision, Graphics, and Image Processing*, vol. 57, no. 2, pp. 227-242, 1993.

[9] T.S. Newman and A.K. Jain, "A Survey of Automated Visual Inspection," *CVGIP Computer Vision, Graphics, and Image Processing*, vol. 61, no. 2, pp. 231-262, 1995.

[10] D.C.W. Pao and H.F. Li, "Shape Recognition Using the Straight Line Hough Transform: Theory and Generalization," *IEEE Trans. Pattern Analysis and Machine Intelligence*, vol. 14, no. 11, pp. 1,076-1,089, 1992.

[11] R. Rosenfeld, J. Ornelas, and Y. Hung, "Hough Transform Algorithms for Mesh-Connected SIMD Parallel Processors," *CVGIP Computer Vision, Graphics, and Image Processing*, vol. 41, no. 3, pp. 293-305, 1988.

[12] T.M. Van Veen, F.C.A. Groen, "Discretization Errors in the Hough Transform," *Pattern Recognition*, vol. 14, pp. 137-145, 1981.